J. Cent. South Univ. (2020) 27: 1146−1157
DOI: https://doi.org/10.1007/s11771-020-4355-5

Springer

Effect of WC grain size on mechanical properties and microstructures of cemented carbide with medium entropy alloy Co-Ni-Fe binder

QIAN Cheng(钱铖)[1], LI Kun(李昆)[1], GUO Xue-yi(郭学益)[2], LIU Bin(刘彬)[1], LONG Zheng-yi(龙郑易)[1], LIU Yong(刘咏)[1]

1. State Key Laboratory of Powder Metallurgy, Central South University, Changsha 410083, China;
2. School of Metallurgy and Environment, Central South University, Changsha 410083, China

Abstract: For developing new binder phase with high performance, Co-Ni-Fe alloy was used as binder in cemented carbides. The mechanical properties of WC-CoNiFe and WC-Co cemented carbides with different grain sizes were studied. The results show that the reprecipitation of WC-CoNiFe is inhibited compared with that of WC-Co during sintering process, and the grains in WC-CoNiFe cemented carbides are more of smooth shape, resulting in a slightly lower hardness and higher transverse rupture strength. With the increase of the grain size, the hardness of the two cemented carbides decreases, and the transverse rupture strength increases. However, the slope values of K in Hall-Petch relationship are higher in WC-CoNiFe than those in WC-Co, indicating the high toughness of medium entropy alloy Co-Ni-Fe.

Key words: cemented carbides; mechanical properties; dissolution-reprecipitation; Hall-Petch relationship; medium entropy alloy

Cite this article as: QIAN Cheng, LI Kun, GUO Xue-yi, LIU Bin, LONG Zheng-yi, LIU Yong. Effect of WC grain size on mechanical properties and microstructures of cemented carbide with medium entropy alloy Co-Ni-Fe binder [J]. Journal of Central South University, 2020, 27(4): 1146−1157. DOI: https://doi.org/10.1007/s11771-020-4355-5.

1 Introduction

Conventional cemented carbides processed by powder metallurgy are based on refractory carbides bonded with a ductile Co phase [1, 2], due to its excellent yield strength, wettability and work hardening properties [3]. However, Co is expensive and scarce in resource, and its toxicity and pollution problems cannot be ignored [4−6]. Therefore, environmentally friendly cemented carbides with good performance and low cost have become an important research area.

New binders for cemented carbides, such as Co-Ni, Ni, Fe, Fe-Ni, have been extensively studied. CHANG et al [7] found that the hardness and the fracture toughness of WC-Ni-Fe were better than those of WC-Co at the same grain sizes. SU et al [8] found that Ni can improve simultaneously the hardness and the fracture toughness of WC-Co-Ni. However, some problems arise using these new binders. For example, although WC-Ni cemented carbides have higher fracture toughness than WC-Co, their hardness and transverse rupture strength are much lower. The grain size of WC-Ni increases easily, and mechanical properties are degraded [9]. On the other hand, the two-phase zone of WC-Fe alloy is very narrow, and the oxidation phenomena are very serious from powder preparation to sintering. The fluctuation of oxygen content causes a little change in the C content, which makes it more difficult to obtain the

Foundation item: Project(51671217) supported by the National Natural Science Foundation of China; Project(2016YFB0700302) supported by the National Key Research and Development Plan of China
Received date: 2019-11-06; **Accepted date:** 2020-03-25
Corresponding author: LIU Yong, PhD, Professor; Tel: +86-13307318308; E-mail: yonliu@csu.edu.cn; ORCID: 0000-0002-6847-9834

two-phase zone of WC-Fe. There is a way to add Ni in Fe binder to improve the mechanical properties [10].

High entropy alloys (HEAs) and medium entropy alloys (MEAs) are multi-component alloys containing several metallic elements (>5 for HEAs and >3 for MEAs) of almost equivalent percentage (5%−35%). These alloys usually have high toughness, high corrosion resistance and high temperature stability. Recently, HEAs and MEAs have been paid much attention on the application as binder phases for cemented carbides. For example, CHEN et al [11] found that the hardness of WC-$Al_{0.5}$CoCrCuFeNi is higher than WC-Co measured both at room temperature and 900 °C. ZHOU et al [12] found that the hardness of the $(FeCoCrNi)_{1-x}(WC)_x$ HEAs composites gradually increases with the increase of WC content from HV 603 to HV 768 at room temperature, and its coefficients of friction (COFs) increase first with the content of WC increasing to 7% then drop. LUO et al [13] found that the average grain size of the WC-10%Al_xCoCrCuFeNi cemented carbides is at least 57% smaller than that of WC-Co with the same processing parameters, due to the sluggish diffusion effect of HEA binders. However, since Cr is a strong carbide-formation element, the stable region for binary (WC-Co) phase is very narrow and it is usually difficult to control the content of carbon in equilibrium. Therefore, medium entropy alloy, CoNiFe is more suitable for acting as a binder of carbides. GAO et al [14] found that the hardness of WC-Co-Ni-Fe increased with the increase of Fe/Ni ratio compared with that of WC-Co. CHANG et al [15] found that nano WC-Co-Ni-Fe possessed superior fracture toughness (K_{IC}) and similar hardness compared with that of nano WC-Co. GILLE et al [16] reported that cemented carbides using the newly developed CoNiFe binder alloys could improve toughness and fatigue strength.

However, most of these studies focused on the influence of the compositions of the new binders on the properties of cemented carbides, and few study was on the effect of WC particle size especially in a wide range. For different particle sizes, the mean free path of binder phase is different, and the size effect of binder phase may be coupled with the compositional effect. Therefore, in this work, the particle size of WC powder is designed from fine (~1 μm) to ultra-coarse (~16 μm) range, and Co-Ni-Fe alloy, instead of Co, was used as binder for cemented carbides.

2 Experimental

2.1 Material preparation

High purity WC of different particle sizes (particle size of 1, 2.3, 4.5, 6, 16 μm), Co (particle size of 1.33 μm), Ni (particle size of 2.0 μm) and Fe (particle size of 3.08 μm) powders were chosen as the staring materials to fabricate WC-5Co-4Ni-1Fe (wt%) (WC-CoNiFe) powders via the sinter hot isostatic pressing (SHIP). WC powders were provided by Xiang Lu Corporation, Co, Ni, Fe powders were provided by GEM. In order to compare the mechanical properties of cemented carbides with new (Co-Ni-Fe) binder and traditional cemented carbide, WC-10Co (wt%) (WC-Co) was also prepared under the same conditions. For convenience, WC-CoNiFe samples with different WC particle sizes are denoted as 1, 2, 3, 4 and 5, respectively, while those of WC–Co are denoted as A, B, C, D and E, respectively. The nominal compositions and WC grain size of WC-CoNiFe and WC-Co were listed in Table 1. The amount of total carbon was adjusted to obtain the desired compositions within the two-phase region. The mixed powders were milled for 24 h in an argon atmosphere in gasoline. The ball-to-powder weight ratio was 4:1, and the rotation rate of the mill was 80 r/min. Subsequently, powders were mixed with 2 wt% paraffin, granulated, sieved and compressed into rectangular specimens. Then, sintering was

Table 1 Nominal compositions (in mass fraction) and WC grain size of WC-CoNiFe and WC-Co composite powders

Sample	Composition/%				WC grain size/μm
	WC	Co	Ni	Fe	
Alloy 1	90	5	4	1	1.0
Alloy 2	90	5	4	1	2.3
Alloy 3	90	5	4	1	4.5
Alloy 4	90	5	4	1	6.0
Alloy 5	90	5	4	1	16.0
Alloy A	90	10	—	—	1.0
Alloy B	90	10	—	—	2.3
Alloy C	90	10	—	—	4.5
Alloy D	90	10	—	—	6.0
Alloy E	90	10	—	—	16.0

performed in a sinter-HIP furnace at 1440 °C for 1 h in Ar atmosphere at a pressure of 5 MPa.

2.2 Mechanical properties test

The name, model and manufacturer of experimental instruments were listed in Table 2. The micro-hardness was measured on a HV-Vicker's hardness instrument using a load of 10 kg and a dwelling time of 10 s. The coercive force (*Hc*) and magnetic saturation (CoM) of the specimens were measured using a SKY-III coercive metre and a ZDMA6535 magnetic saturation.

Table 2 Name, model and manufacturer of experimental instruments

Instrument	Model	Manufacturer
HV-Vicker	BUEHLER5104	Buehler
Coercive meter	SKY-III	Changsha Xianyou Electronic Scientific Development Co., Ltd.
Magnetic saturation induction tester	ZDMA6535	Changsha Zhongda Precision Instruments Co., Ltd.
Dynamic and static electro-hydraulic servo testing machine	8802	Instron
Scanning electron microscope	Quanta FEG 250	FEI
X-ray diffractometer	D/MAX-2250	Rigaku
Electron probe microanalysis	JXA–8230	JEOL

3 Results

3.1 Microstructure

Figure 1 shows the microstructures of WC-CoNiFe and WC-Co. Figures 1(a)−(e) show the microstructures of WC-Co, and Figures 1(f)−(j) show the microstructures of WC-CoNiFe. All samples are composed of WC phase and binder phase, which are evenly distributed. The η phase and graphite phase are not present. Figures 1(f)−(j) show that the shape of WC changes with the particle size. When the original particle size of WC is smaller than 6 μm, the shape of WC is irregular. With the increase of the size, the shape of WC becomes smooth. However, in Figures 1(a)−(e), the shape of WC in WC-Co does not change with the original size of WC, and it is always irregular.

The mean grain size of WC and the mean free path (MFP) of Co in cemented carbides were measured by using the intercept method. The results are shown in Table 3. Due to the disintegration of particles during ball milling, the mean grain size of WC is smaller than that of the original powder, except for that the cemented carbide using the smallest size of the original powder (1 μm) has an increased grain size. As the particle size of the original powder increased, the decrease of WC size after sintering becomes obvious. It can also be found that the mean grain size of WC and the MFP of Co in WC-CoNiFe is slightly lower than those of the WC-Co with the same binder content and original powder size. Combining with Figure 1, it is found that the mean grain size of WC of the sintered WC-CoNiFe is smaller and the shape is smoother than WC-Co under the same particle size of the original powder.

The grain size distributions of WC in WC-CoNiFe with different raw particle sizes are presented in Figure 2. Except Alloy 1, which has a larger grain size of WC than that in original powder (1 μm), due to the disintegration of particles during ball milling, the mean grain size of WC decreases compared with original powder. Alloy 5 (Figure 2(e)) has the widest grain size distribution (0.5−10.5 μm) due to the largest raw particle size. The grain size distributions of the five groups of samples are of a single-model parabolic manner. The mean grain size is taken from the peak position of different curves.

Figure 3 presents the XRD patterns of WC-CoNiFe and WC-Co cemented carbides. Both cemented carbides are composed of WC phase and binder phase. There are no η phase and graphite phase. The binder phases all have a face-centered cubic (FCC) structure, and the three peaks of them from left to right are (111), (200) and (220). However, the values of 2θ are different, and the lattice constant of Co-Ni-Fe is 3.560 Å, while Co is 3.554 Å. It shows that the peaks of Co-Ni-Fe phase change compared with Co phase due to solid solution effects. The three main peaks of WC from left to right are (001), (100), (101) and the relative intensity ratios for $I_{(001)}/I_{(100)}$ and $I_{(101)}/I_{(100)}$ are listed in Table 4. Compared with WC-Co, the ratio of $I_{(001)}/I_{(100)}$ of WC-CoNiFe decreases and that of $I_{(101)}/I_{(100)}$ increases. As mentioned by ZHANG et al [18], this characteristic indicates that the shape of WC grains increases to nearly round.

The distribution of binder phase of WC-CoNiFe is shown in Figure 4. It can be seen

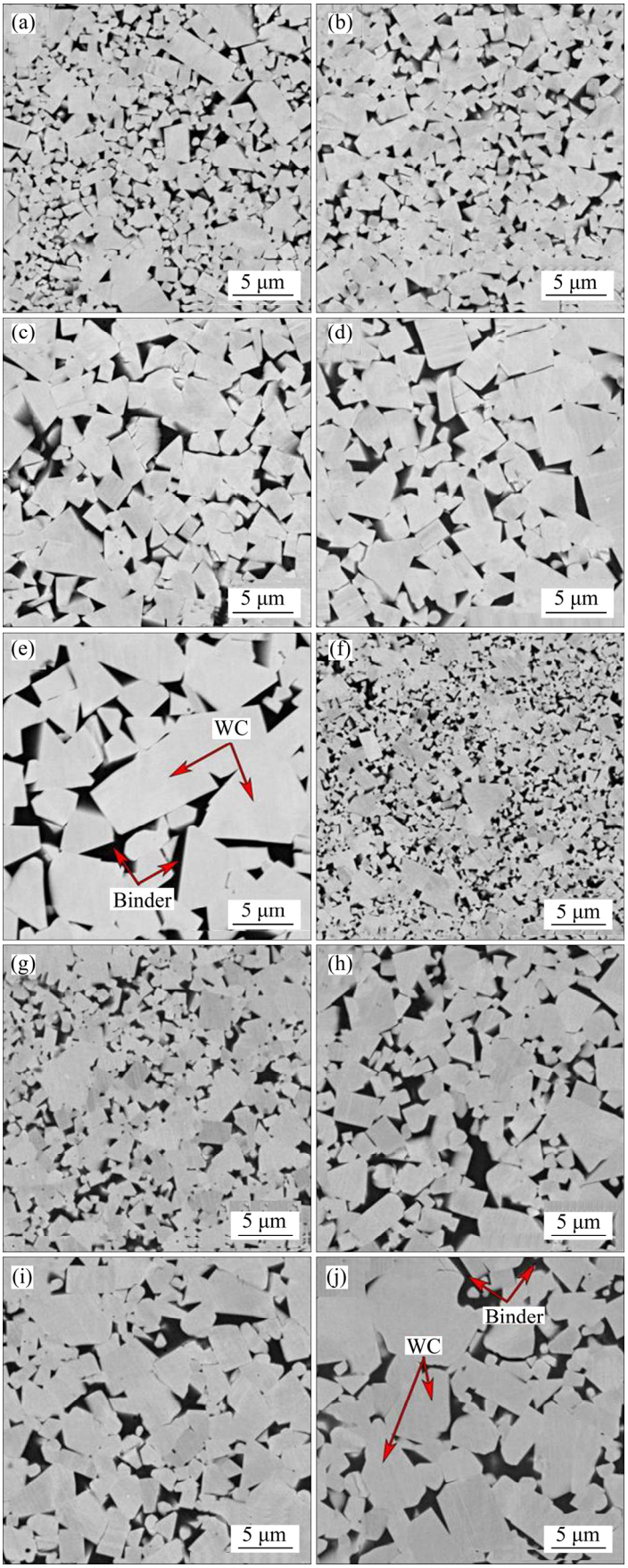

Figure 1 Microstructures of WC-Co: (a) Alloy A; (b) Alloy B; (c) Alloy C; (d) Alloy D; (e) Alloy E; and Microstructures of WC-CoNiFe: (f) Alloy 1; (g) Alloy 2; (h) Alloy 3; (i) Alloy 4; (j) Alloy 5

Table 3 Particle size of initial WC in raw powder, mean grain size of WC and mean free path (MFP) of Co in sintered cemented carbides

Sample	WC size in powder/μm	Mean grain size of WC/μm	MFP/μm
Alloy 1	1.0	1.32±0.05	0.150
Alloy 2	2.3	2.03±0.13	0.317
Alloy 3	4.5	3.65±0.12	0.637
Alloy 4	6.0	4.19±0.05	0.873
Alloy 5	16	6.25±0.21	1.168
Alloy A	1.0	1.38±0.08	0.204
Alloy B	2.3	2.08±0.08	0.325
Alloy C	4.5	3.79±0.05	0.667
Alloy D	6.0	4.32±0.19	0.985
Alloy E	16.0	6.62±0.26	1.298

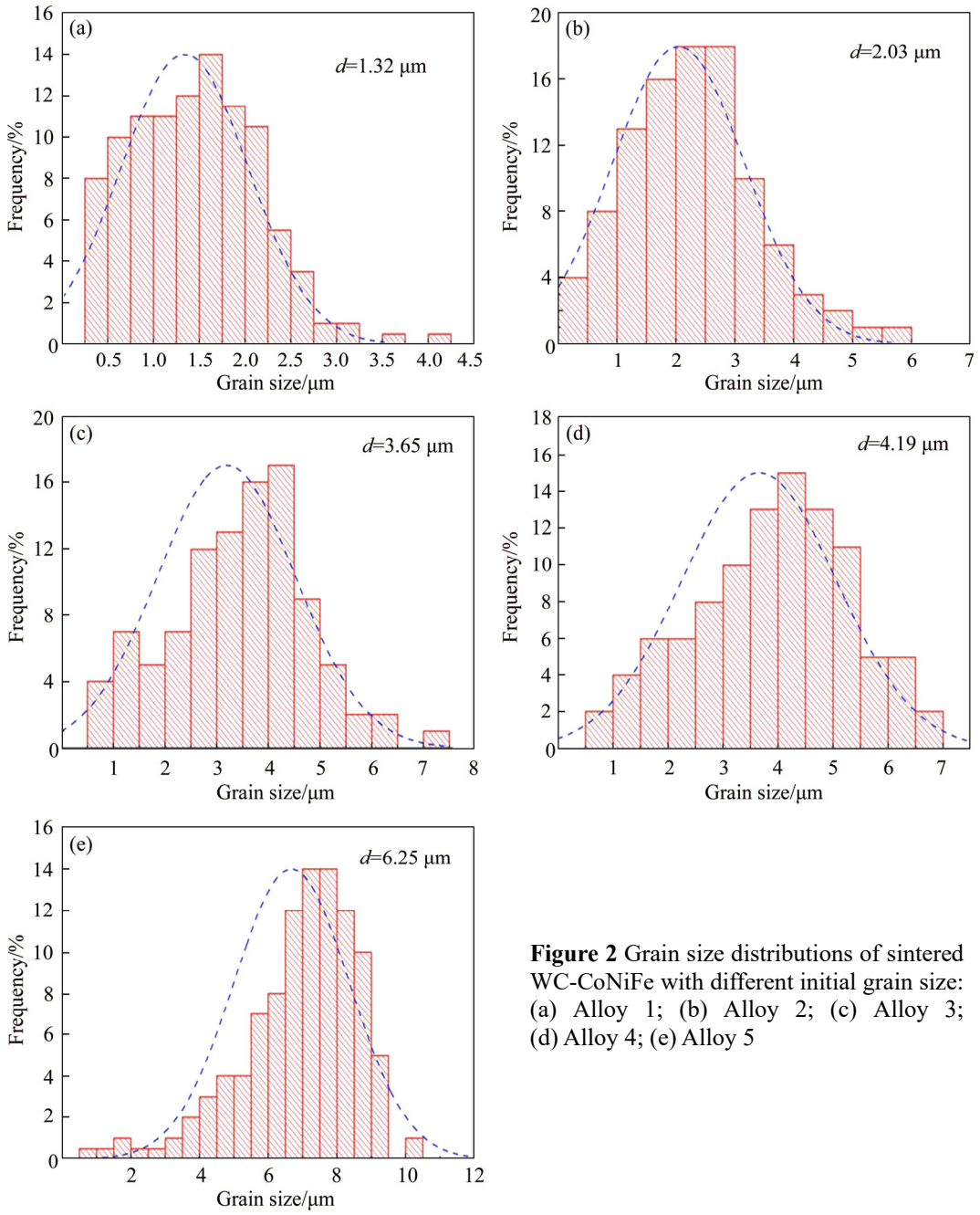

Figure 2 Grain size distributions of sintered WC-CoNiFe with different initial grain size: (a) Alloy 1; (b) Alloy 2; (c) Alloy 3; (d) Alloy 4; (e) Alloy 5

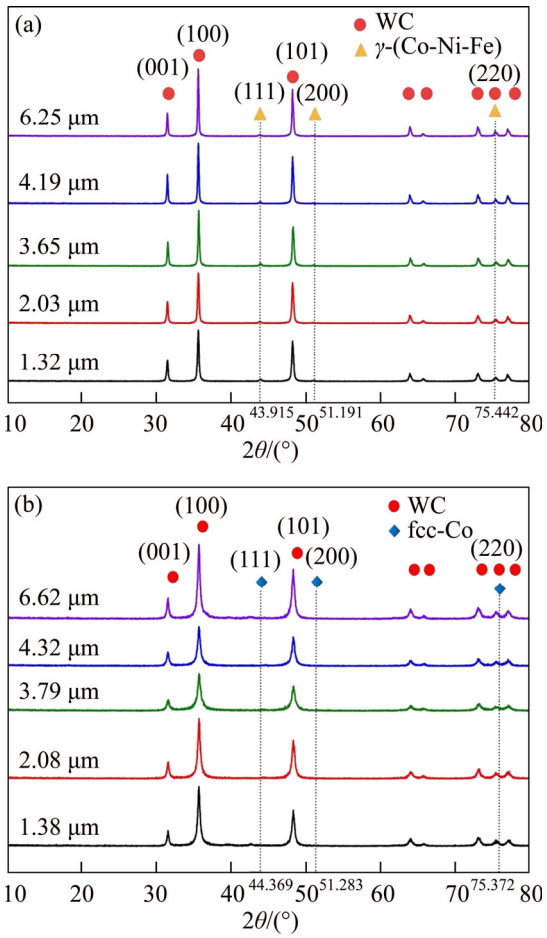

Figure 3 XRD patterns of WC-CoNiFe (a) and WC-Co (b)

Table 4 Relative intensity ratios of WC grain planes extracted from WC-CoNiFe and WC-Co cemented carbides

Sample	$I_{(001)}/I_{(100)}$	$I_{(101)}/I_{(100)}$
Alloy 1	0.440	0.882
Alloy 2	0.440	0.882
Alloy 3	0.440	0.882
Alloy 4	0.440	0.882
Alloy 5	0.440	0.882
Alloy A	0.444	0.842
Alloy B	0.444	0.842
Alloy C	0.444	0.842
Alloy C	0.444	0.842
Alloy E	0.444	0.842

that the elements of Co, Ni and Fe distribute evenly around WC. The contents of Co and Ni are high and the content of Fe is low. Except for a few areas with relatively higher content of binder phase, the binder phase is basically uniform in distribution.

3.2 Magnetic properties

The saturation magnetization (M_{sat}) and the magnetic coercivity (H_C) of the WC-CoNiFe and WC-Co cemented carbides are shown in Table 5. It can be seen that M_{sat} and H_C of the WC-CoNiFe are lower than those of WC-Co cemented carbide on the premise of the same particle size of the original powder. M_{sat} is related to the composition of the binder or the amount of W dissolved in the Co binder [8]. The order of the magnetic saturation is: Fe (217 μT·m^3/kg) > Co (161 μT·m^3/kg) > Ni (54.8 μT·m^3/kg) [15]. In the new binder of CoNiFe, the magnetic saturation is smaller than pure cobalt. Moreover, the solubility of WC in CoNiFe is higher than that in Co, and there is much W dissolving in the binder phase, resulting in a lower M_{sat} . For WC-Co cemented carbides, a commonly accepted empirical relationship between the microstructural parameters and H_C is [8, 19]:

$$H_C=1.44+0.04m_{Co}+\frac{12.47-0.37m_{Co}}{d_{WC}} \quad (2)$$

where H_C is the magnetic coercivity; d_{WC} is the mean WC grain size; m_{Co} is the mass fraction of Co in the composite.

H_C is related to the grain size of WC(d_{WC}) and the content of binder phase. The effects of the grain size of WC on the magnetic coercivity (H_C) are shown in Figure 5. At the same binder composition, H_C decreases with the increase of WC particle size. At the same WC particle size, the H_C of cemented carbide with new (CoNiFe) binder is lower than that of WC-Co cemented carbide.

3.3 Mechanical properties

Figure 6(a) presents the hardness of the WC-CoNiFe and WC-Co cemented carbides with the increasing particle size of WC powder. It can be seen that at the same binder content, the hardness is inversely proportional to the particle size of WC powder, and decreases with the increase of particle size. The hardness of WC-Co cemented carbide is higher than that of WC-CoNiFe with the same particle size of WC powder.

Figure 6(b) presents the TRS of the WC-CoNiFe and WC-Co cemented carbides with the increasing particle size of WC powder. The TRS is proportional to the particle size of the original powder at the same binder content, and increases with the increase of particle size.

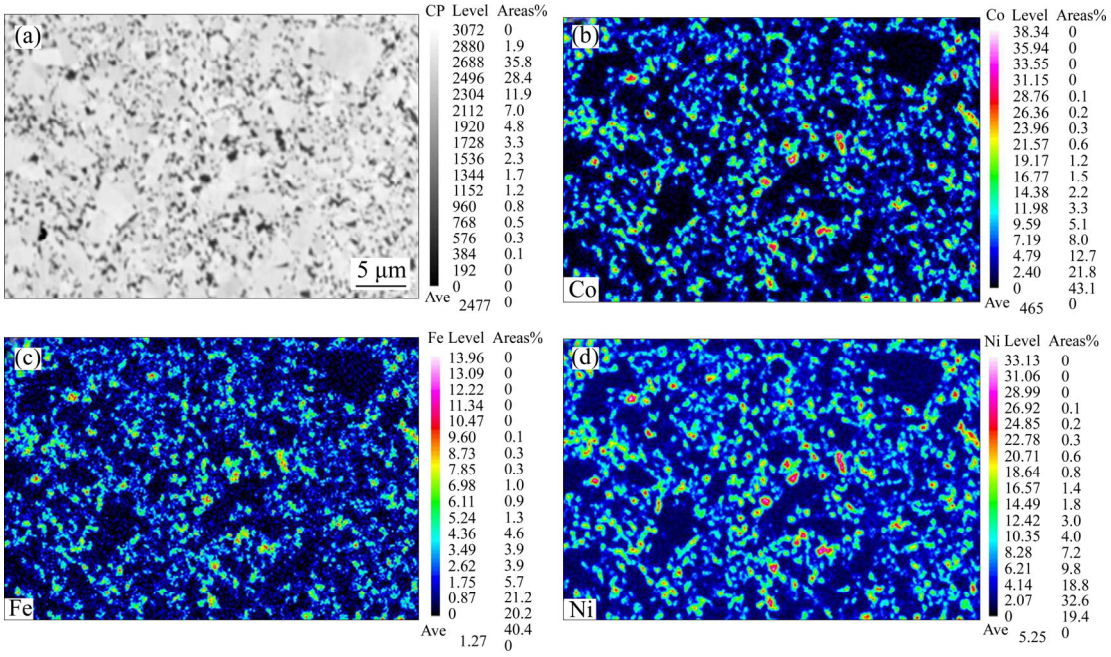

Figure 4 Compositional distribution of binder phase in WC-CoNiFe, microstructure (a), Co (b), Fe (c) and Ni (d)

Table 5 Magnetic properties and mechanical properties of WC-CoNiFe and WC-Co cemented carbides

Sample	Magnetic saturation/%	Coercivity, H_c/(kA·m^{-1})	Hardness (HV)	TRS/MPa
Alloy 1	6±0.12	11.2±0.04	1506±20.4	1772±32
Alloy 2	5.8±0.03	6.7±0.02	1419±29.7	2170±29
Alloy 3	5.6±0.07	5±0.03	1274±23.3	2658±38
Alloy 4	5.9±0.03	4.7±0.04	1258±22.2	2994±35
Alloy 5	5.5±0.04	4.2±0.04	1167±16.8	3213±36
Alloy A	8±0.12	12.5±0.12	1605±19.5	1677±35
Alloy B	7.3±0.06	10.4±0.03	1519±13.2	1952±34
Alloy C	7.4±0.03	7.6±0.03	1356±17.6	2554±37
Alloy D	7.6±0.03	7.2±0.05	1340±17.2	2881±38
Alloy E	7.7±0.04	4.9±0.03	1195±28.4	3155±34

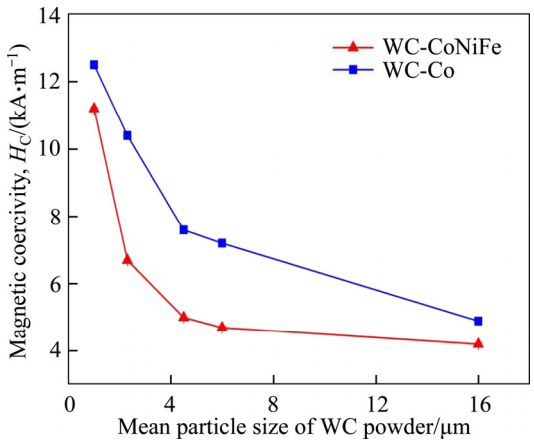

Figure 5 Effects of WC grain size on magnetic coercivity (H_C)

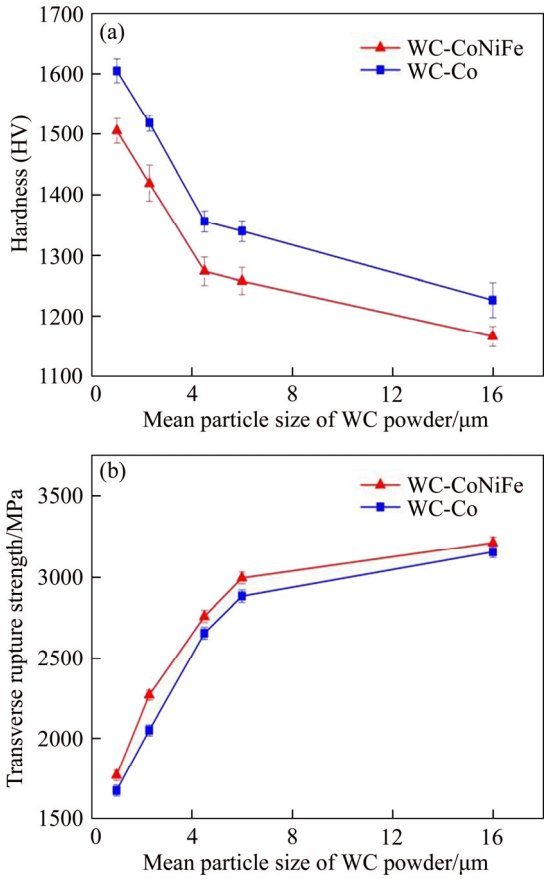

Figure 6 Hardness and TRS of WC-CoNiFe and WC-Co cemented carbides VS grain size of original WC powder: (a) Hardness; (b) TRS

Moreover, the TRS of cemented carbide with new (Co-Ni-Fe) binder increases by about 5% than that

of WC-Co cemented carbide at the same particle size of WC powder.

The SEM images of fracture surface of the TRS specimens with different grain sizes are presented in Figure 7. The weakest part of cemented carbide is the interface between WC grains, followed by WC grain, WC-Co phase interface and cobalt layer. Therefore, there are four microstructural fracture modes of cemented carbide: intergranular fracture (C/C) along WC/WC grains, transgranular fracture (C) through WC grains, fracture along the inner surface between WC and binder phases (C/B), and ductile fracture (B) through binder phases [15, 20]. In Alloy 1 (Figure 7(a)), 90% of the fracture sites are intergranular (C/C) with smooth surface along WC/WC grain boundary, and there are fewer transgranular fracture sites (C) and much less ductile fractures (B) passing through the binder phase. At the same time, C/B fractures extending along WC/Co interface could hardly be seen. In Alloy 2 (Figure 7(b)), the fracture sites are mainly C/C, C-type fractures increase, and a small portion of B-type and C/B fractures occur. With the increase of the grain size, in Alloy 3−Alloy 5 (Figures 7(c)−(e)), C/C fractures decrease, C, B and C/B fractures increase gradually. In Alloy 5 (Figure 7(e)), the dimple pattern (B) of honeycomb is relatively large in size, accounting for more than 25%, showing obvious ductile fracture of Co phase. Therefore, the fracture morphology further reflects that the toughness of cemented carbide increases with the increase of grain size, and the toughness of cemented carbide with new (CoNiFe) binder is better than that of WC-Co cemented carbide.

4 Discussion

4.1 Microstructural evolution

Compared with WC-Co, WC-CoNiFe has a smaller WC grain size, and smoother shape of WC grain. The differences in grain size and shape of WC are explained as follows.

According to the vertical section of the C-Co-Fe-Ni-W system, the liquid phase temperature of WC-CoNiFe is higher than that of WC-Co [21], so the dwell time in liquid phase (γ phase) of the new binder is shorter. The growth of grains during sintering depends on the dissolution-reprecipitation process, and the decrease of interfacial energy is the main driving force [22, 23]. Shorter duration of γ phase leads to lower driving force of dissolution-reprecipitation process in sintering process, thus inhibiting the reprecipitation of WC grains and resulting in the decrease of the grain size.

WC belongs to the simple hexagonal system (type P-6m2). Each unit cell has a W atom and a C atom. The C atom occupies an asymmetric position (1/3, 2/3, 1/2) in the unit crystal system [24, 25]. SCHUBERT et al [24] found that due to the asymmetric occupancy of C atoms, the unbalanced "growth" of WC crystal resulted in the formation of the trigonal prism, the triangular plate and the hexagonal plate WC. These types of WC have sharp boundaries and are not considered to be round. Alternative binder systems, such as Fe, Fe-Cr, Ni-Cr or Co-Ni-Cr can contribute to inhibit shape transformation of the WC grains in comparison to the Co system, for examples, there is a strong growth inhibition effect of the iron binder [26]. The presence of Fe in the new binder can inhibit the unbalanced growth of WC, so the WC grain in the new binder is more of nearly-round shape than that of the WC-Co cemented carbide. Meanwhile, as WC grain size increases, the surface-to-volume ratio and the volume fraction of grain boundaries become smaller, resulting in lower interfacial energy [27], i.e., lower driving force for the reprecipitation of WC. Therefore, with the increase of WC grain size, the shape of sintered WC grain is more of smooth shape.

4.2 Mechanical properties

It is found that the hardness of WC-CoNiFe is lower than that of WC-Co at the same particle size of WC powder, but the TRS of WC-CoNiFe is higher. Moreover, with the increase of particle size, the hardness decreases and the TRS increases. The differences in mechanical properties are explained as follows.

The hardness of cemented carbide is determined by the mean grain size and the composition of binder. It is well found that the hardness increases with the decrease of WC particle size. On the other hand, the hardness values (HB) of Co, Ni and Fe are: Co (125) > Ni (80) > Fe (50). Some studies have shown the same decreasing trend of hardness in WC-10Co, WC-10Ni and WC-10Fe [28]. Moreover, the hardness decreases with the

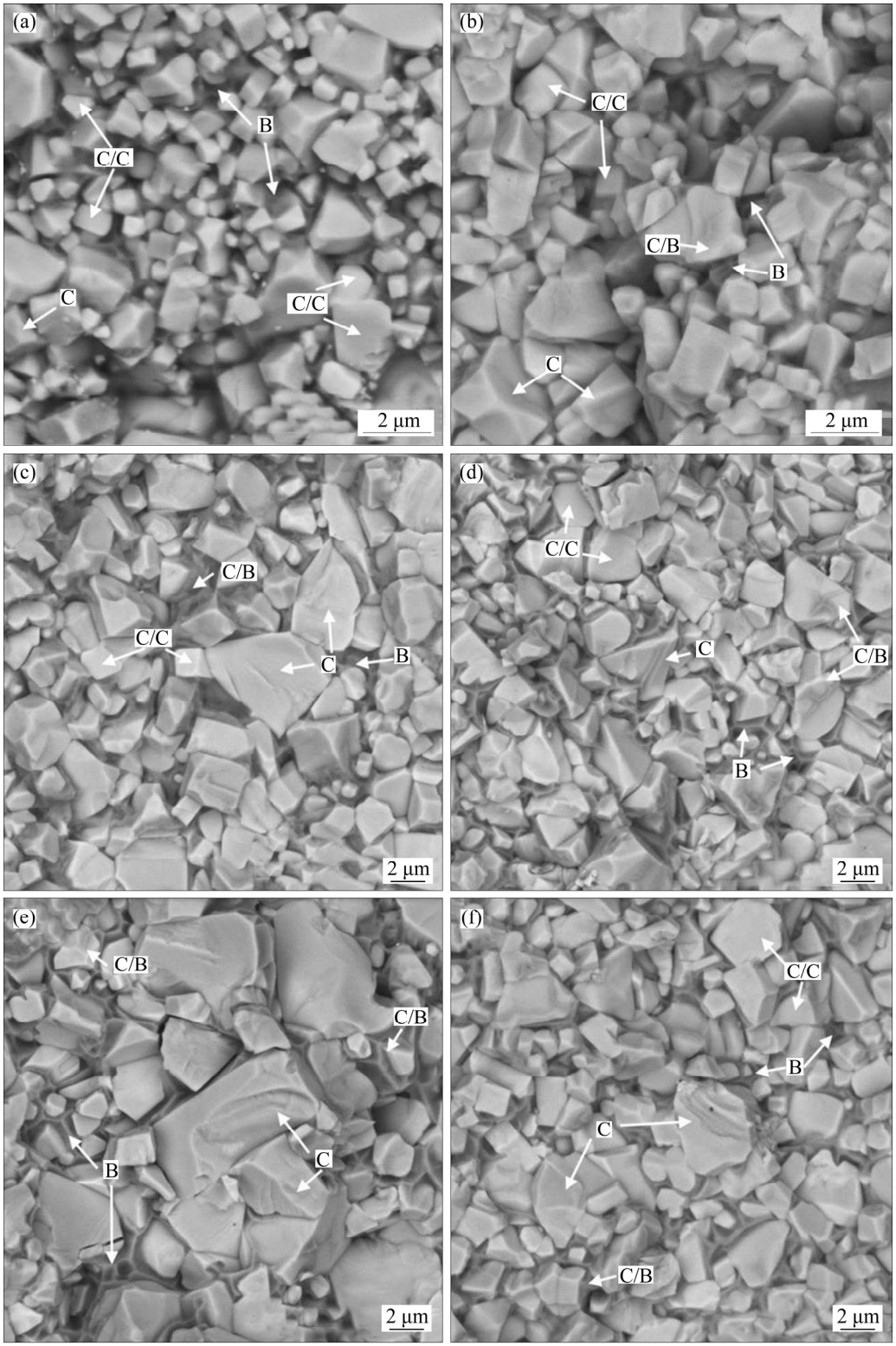

Figure 7 SEM images of fracture surface of TRS specimens with different grain size: (a)−(e) Alloy 1−Alloy5; (f) Alloy D

increase of Ni content and increases with the increase of Fe content. Meanwhile, the atomic radius and the valence electron number of Co and Ni are similar, so the solid solution strengthening effect of Co-Ni-Fe is very weak. In this work, the addition of Ni decreases the hardness of binder phase, and the small addition of Fe does not contribute to increase the hardness. Therefore, the hardness of WC-CoNiFe is less than that of WC-Co due to decreased content of Co.

The TRS reflects both the hardness and the toughness of materials. With the increase of grain size, the MFP of Co increases correspondingly, as shown in Table 3. A large MFP of Co reduces the stress concentration through plastic deformation, and the generation and propagation of cracks are hindered, resulting in an increase in TRS [29]. Therefore, in a certain range of particle size, the TRS is proportional to the particle size of the original powder when the binder content is the same. Some studies [28, 30] showed that the plasticity of WC-Ni is better than that of WC-Co. At the same time, because the WC grain is of nearly-round shape in WC-CoNiFe, local stress concentration effect caused by sharp boundary, which occurs in WC-Co, is released to a large extent [31], the crack propagation is more difficult, and TRS is slightly higher.

The Hall-Petch (H-P) relationships of hardness and TRS in the WC-CoNiFe and WC-Co are shown in Figure 8. It shows that the hardness and TRS of both cemented carbides are in good agreement with Hall-Petch relationship [32, 33]. The equations are also shown in Figure 8.

The hardness values of the WC-CoNiFe are smaller than those of the WC-Co cemented carbides in all the particle size range. Moreover, it is found that the values of K for hardness and TRS of WC-Co are larger than those of WC-CoNiFe, i.e., the effects of the grain size on the hardness and TRS of WC-Co are greater than those on WC-CoNiFe. The value of K is related to the type of materials. ROA et al [33] found that the K value in H-P relationship of cemented carbides is between those of WC and Co, and WC-Co cemented carbides have a two-phase Hall-Petch relationship effect. Therefore, the better the toughness of cemented carbide, the smaller the absolute value of K. Moreover, the value of K is also an effective indication that the toughness of WC-CoNiFe is better than that of WC-Co.

5 Conclusions

The CoNiFe binder phase can inhibit the reprecipitation process of WC during liquid phase sintering, resulting in a smooth morphology and slow grain growth rate of WC grains.

Due to the smooth WC grains and high toughness of CoNiFe alloy, the WC-CoNiFe cemented carbides have a lower hardness but higher transverse rupture strength than WC-Co cemented carbides when the grain size of WC is the same.

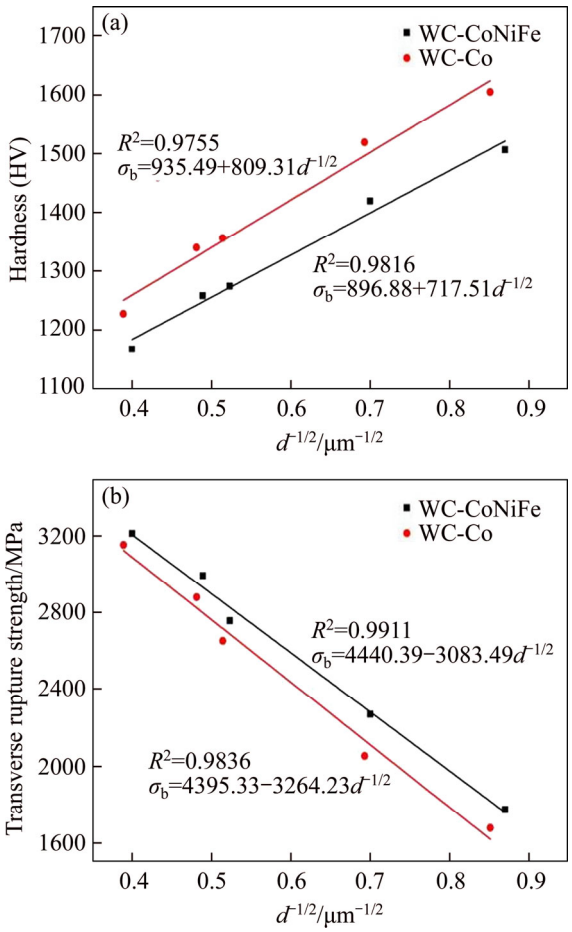

Figure 8 Hall-Petch relationships of hardness and TRS in WC-CoNiFe and WC-Co: (a) Hardness; (b) TRS

The slope values of K, in the H-P relationships of hardness and transverse rupture strength, of WC-CoNiFe are smaller than those of WC-Co cemented carbides, indicating a high toughness of CoNiFe medium entropy alloy.

References

[1] KONYASHIN I, HLAWATSCHEK S, RIES B, LACHMANN F, VUKOVIC M. Cobalt capping on WC−Co hardmetals. Part I: A mechanism explaining the presence or absence of cobalt layers on hardmetal articles during sintering [J]. International Journal of Refractory Metals & Hard Materials, 2014, 42(1): 142−150.

[2] NAN L, HE Y, JIN Z. Enhanced mechanical properties and oxidation resistance of tungsten carbide-cobalt cemented carbides with aluminum nitride additions [J]. Ceramics International, 2017, 43(8): 6603−6606.

[3] GARCIA J. Influence of Fe−Ni−Co binder composition on nitridation of cemented carbides [J]. International Journal of

Refractory Metals & Hard Materials, 2012, 30(1): 114−120.
[4] ZHAO Z, LIU J, TANG H, MA X, ZHAO W. Investigation on the mechanical properties of WC−Fe−Cu hard alloys [J]. Journal of Alloys & Compounds, 2015, 632: 729−734.
[5] FERNANDES C M, VILHENA L M, PINHO C M S, OLIVEIRA F J, SOARES E, SACRAMENTO J, SENOS A M R. Mechanical characterization of WC–10 wt% AISI 304 cemented carbides [J]. Materials Science and Engineering A, 2014, 618(4): 629−636.
[6] LINDER D, HOU Z, XIE R, HEDSTRÖM P, STRÖM V, HOLMSTRÖM E, BORGENSTAM A. A comparative study of microstructure and magnetic properties of a Ni Fe cemented carbide: Influence of carbon content [J]. International Journal of Refractory Metals and Hard Materials, 2019, 80: 181−187.
[7] CHANG S H, CHEN S L. Characterization and properties of sintered WC−Co and WC−Ni−Fe hard metal alloys [J]. Journal of Alloys and Compounds, 2014, 585: 407−413.
[8] SU W, WEN Y, ZHANG Q. Effects of Ni and Cu additions on microstructures, mechanical properties and wear resistances of ultra-coarse grained WC−6Co cemented carbides [J]. International Journal of Refractory Metals and Hard Materials, 2018, 70(1): 176−183.
[9] ZHANG F G, ZHU X P, LEI M K. Surface characterization and tribological properties of WC-Ni cemented carbide irradiated by high intensity pulsed electron beam [J]. Vacuum, 2017, 137(3): 119−124.
[10] CAI X, ZHONG L, XU Y, LI X, LIU M. Microstructure and fracture toughness of a WC-Fe cemented carbide layer produced by a diffusion-controlled reaction [J]. Surface and Coatings Technology, 357(1): 784−793.
[11] CHEN C S, YANG C C, CHAI H Y, YEH J W, CHAU J L H. Novel cermet material of WC/multi-element alloy [J]. International Journal of Refractory Metals and Hard Materials, 2014, 43(12): 200−204.
[12] ZHOU R, CHEN G, LIU B, WANG J W, HAN L L, LIU Y. Microstructures and wear behaviour of $(FeCoCrNi)_{1-x}(WC)x$, high entropy alloy composites [J]. International Journal of Refractory Metals and Hard Materials, 2018, 75: 56−62.
[13] LUO W, LIU Y, SHEN J. Effects of binders on the microstructures and mechanical properties of ultrafine WC-10%AlxCoCrCuFeNi composites by spark plasma sintering [J]. Journal of Alloys and Compounds, 2019, 791: 540−549.
[14] GAO Y, LUO B H, HE K J, ZHANG W W, BAI Z H. Effect of Fe/Ni ratio on the microstructure and properties of WC-Fe-Ni-Co cemented carbides [J]. Ceramics International, 2018, 44(2): 2030-2041.
[15] CHANG S H, CHANG M H, HUANG K T. Study on the sintered characteristics and properties of nanostructured WC–15 wt% (Fe−Ni−Co) and WC–15 wt% Co hard metal alloys [J]. Journal of Alloys and Compounds, 2015, 649: 89−95.
[16] GILLE G, BREDTHAUER J, GRIES B, MENDE B, HEINRICH W. Advanced and new grades of WC and binder powder–their properties and application [J]. International Journal of Refractory Metals & Hard Materials, 2000, 18(2, 3): 87−102.
[17] BS EN ISO 3327:2009. Hardmetals-determination of transverse rupture strength [S]. Brussels: European Committee for Standardization, 2009.
[18] ZHANG L, TIAN W, CHEN Y, LIU T, ZHANG H D, ZHOU L, ZHU J F. Fine platelet-like grained WC−Co cemented carbides: Preparation, characterization, properties and application in PVD coating substrates [J]. International Journal of Refractory Metals and Hard Materials, 2017, 64(Complete): 135−142.
[19] ROEBUCK B, GEE M, BENNETE G, MORRELL R. Measurement good practice guide No. 20−Mechanical tests for hardmetals [R]. National Physics Laboratory, 2009 (ISSN 1368-6550).
[20] LLANES L, TORRES Y, ANGLADA M. On the fatigue crack growth behavior of WC−Co cemented carbides: Kinetics description, microstructural effects and fatigue sensitivity [J]. Acta Materialia, 2002, 50(9): 2381−2393.
[21] ZHOU P, LIU S, WANG P, XU H, PENG Y, YUAN X, DU Y, ZHANG J, HUANG W. Experimental investigation and thermodynamic assessment of the Hf-Mn system [J]. Journal of Phase Equilibria and Diffusion, 2011, 33(1): 20−28.
[22] CHANG S H, CHANG P Y. Investigation into the sintered behavior and properties of nanostructured WC−Co−Ni−Fe hard metal alloys [J]. Materials Science and Engineering A, 2014, 606: 150−156.
[23] CHANG S H, CHEN S L. Characterization and properties of sintered WC−Co and WC−Ni−Fe hard metal alloys [J]. Journal of Alloys and Compounds, 2014, 585: 407−413.
[24] HERBER R P, SCHUBERT W D, LUX B. Hardmetals with “rounded” WC grains [J]. International Journal of Refractory Metals & Hard Materials, 2006, 24(5): 360−364.
[25] KIM S, HAN S H, PARK J K, KIM H E. Variation of WC grain shape with carbon content in the WC−Co alloys during liquid-phase sintering [J]. Scripta Materialia, 2003, 48(5): 635−639.
[26] WITTMANN B, SCHUBERT W D, LUX B. WC grain growth and grain growth inhibition in nickel and iron binder hardmetals [J]. International Journal of Refractory Metals & Hard Materials, 2002, 20(1): 51−60.
[27] ZHAO S, SONG X, ZHANG J, LIU X. Effects of scale combination and contact condition of raw powders on SPS sintered near-nanocrystalline WC−Co alloy [J]. Materials Science and Engineering A, 2008, 473(1, 2): 323−329.
[28] SHON I J, JEONG I K, KO I Y, DOH J M, WOO K D. Sintering behavior and mechanical properties of WC–10Co, WC–10Ni and WC–10Fe hard materials produced by high-frequency induction heated sintering [J]. Ceramics International, 2009, 35(1): 339−344.
[29] EXNER H E, GURLAND J. A review of parameters influencing some mechanical properties of tungsten carbide-cobalt alloys [J]. Powder Metallurgy, 1970, 13(25): 13−31.
[30] GAO Y, LUO B H, BAI Z H, ZHU B, OUYANG S. Effects of deep cryogenic treatment on the microstructure and properties of WC[sbnd]Fe[sbnd]Ni cemented carbides [J]. International Journal of Refractory Metals & Hard Materials, 2016, 58: 42−50.
[31] SCHUBERT W D, FUGGER M, WITTMANN B, USELDINGER R. Aspects of sintering of cemented carbides with Fe-based binders [J]. International Journal of Refractory

Metals and Hard Materials, 2015, 49: 110−123.
[32] ARMSTRONGRW. 60 years of Hall-Petch: past to present nano-scale connections [J]. Mater Trans, 2014, 55: 2−12.
[33] ROA J J, JIMÉNEZ-PIQUÉ E, TARRAGÓ, JM, SANDOVAL D A, MATEO A, FAIR J, LLANES L. Hall-Petch strengthening of the constrained metallic binder in WC−Co cemented carbides: Experimental assessment by means of massive nanoindentation and statistical analysis [J]. Materials Science and Engineering A, 2016, 676: 487−491.

(Edited by HE Yun-bin)

中文导读

WC 晶粒尺寸对中熵合金(Co-Ni-Fe)粘结剂硬质合金力学性能和微观组织的影响

摘要：为了开发高性能的新型粘结相，Co-Ni-Fe 合金被用作硬质合金中的粘结剂。本文研究了不同晶粒尺寸的 WC-CoNiFe 与 WC-Co 的力学性能的差异。结果表明，与 WC-Co 相比，在烧结过程中 WC-CoNiFe 的再沉淀得到抑制，WC 晶粒更平整，造成硬度略低，抗弯强度增强。并且随着晶粒尺寸的变大，两种硬质合金的硬度变低，抗弯强度上升。而且，在霍尔-佩奇关系中，WC-CoNiFe 的斜率值 *K* 高于 WC-Co，表明中熵合金 Co-Ni-Fe 具有较高的韧性。

关键词：硬质合金；力学性能；溶解-再析出；霍尔-佩奇关系；中熵合金